

Experimental investigation and numerical simulation of instabilities in a multi-parallel channel two-phase natural circulation system

LS Sangweni^a and RT Dobson^b

Department of Mechanical and Mechatronic Engineering, University of Stellenbosch, Stellenbosch, South Africa
Private Bag X1, Matieland 7602, South Africa

Abstract

In the present study, two-phase natural circulation flow in a multi-parallel channel system is investigated using experimental and numerical modelling. The experimental model consisted, essentially, of four 25 mm diameter and two-meter long vertically orientated transparent polycarbonate pipes connected to a common manifold at the bottom and a relatively large steam drum at the top; three one-meter long electrical resistance heating elements were inserted into the lower end of three of the vertical pipes. Tests were conducted using different combinations of input power and as-defined and so-called open, closed and heat pipe system operating modes. A water-cooled condenser was placed in the upper portion of the steam drum and an expansion tank was connected to the lower manifold. For different power inputs and operating modes twelve temperatures and three flow rates as a function of time were recorded. In this way start-up transients and dynamical oscillatory responses were captured. So-called Type I instability were observed at low power inputs and open system operating modes (system open to the atmosphere). Type II instabilities and flashing instability were observed at medium and high-power excitations for the open system mode of operation. The fluid flow became more stable and less oscillatory at all power excitations for the closed system operation mode (system not open to the atmosphere). For the heat pipe mode of operation so-called geysering, followed by flashing-induced boiling was observed. After boiling had commenced downward single phase flow was invariable noted to occur in the central of the three heated risers, even when all three heater power inputs were the same. Also, after boiling had started a further increase in power input did not necessarily result in an increase in flow rate.

The experimental system was discretized into a number of control volumes. The conservation equations, mass, momentum and energy were applied to each control volume and a set of time dependent temperature-coupled finite difference equations simulating the thermal-hydraulic behaviour of the system thus derived. This set of difference equations was solved using an explicit solution method. An encouragingly-good correspondence between the experimental and theoretical simulation model of the temperature and flow rate in the system was obtained.

Keywords: Multi-channel natural circulation loop, Two-phase flow, Transient response, Flow instabilities, Thermal-hydraulic simulation

1. Introduction

Natural circulation loops are capable of transporting heat passively from a heat source to a heat sink utilizing natural forces such as convection and gravity. For this reason, natural circulation loops enhance safe operation and reliability as opposed to mechanical pumped systems. For this reason, such systems are greatly utilized in many industrial systems, e.g. solar heaters, nuclear power plants, energy conversions and thermal control of electronic components (Swapnalee and Vijayan, 2011:54).

However, natural circulation loops are susceptible to various instabilities during operation. Instabilities in a natural circulation system are undesirable as they can hinder safe operation of plants. Flow instabilities in water-cooled and water moderated industrial systems are of particular importance since they can cause problems of system control and mechanical vibrations of components hence must be avoided

(Zhang et al., 2009).

Most commercial energy-generation systems utilizing natural circulation boiling consist of many parallel channels connected between common plena. The presence of multiple channels poses many challenges, as it triggers various modes of flow instability that need to be overcome by proper design and operating procedures (Jain et al., 2010:34).

This study carries on from work done by Ruppertsberg (2008) and White (2011). In their studies, both Ruppertsberg and White worked on a single loop single-phase flow and double loop two-phase flow natural circulation system respectively, investigating and modelling the instabilities of such systems.

^aTel: 27 73 951 7239; E-mail: Lucy.Sangweni@gmail.com

^bTel: 27 808 4268; Fax: 0866 155 206; E-mail: rtd@sun.ac.za

In this context, a parallel channel loop has been designed and built to investigate the instabilities of a multi-channel thermosyphon loop. The loop comprises three identical parallel channels connected between a steam drum and header. A single down-comer connected between two common plenums, i.e. steam drum and header, provides the recirculation path. The multi-channel natural circulation system was also simulated theoretically. Detailed flow and stability experiments were undertaken at various operating conditions. The experimental response characteristics recorded in this manner were compared with the analytical model's results, and thereby the accuracy with which the analytical model simulates the experimental results was established.

2. Experimental Investigation

One of the objectives of this study was to perform practical investigations of the instabilities of single- and two-phase flows in a multi-channel thermosyphon loop. To achieve this goal, a four parallel-channel natural circulation loop was designed, constructed and tested.

2.1. Experimental design

In this context, a parallel channel loop was designed and built to investigate the instabilities of a multi-channel thermosyphon loop. Three heating sections were chosen based on the conclusion drawn by Lee and Pan (1999:32), which states that "a 3 channels plus system exhibits instability characteristics fairly similar to a 2-channel system". White (2011) performed an investigation of two-phase flow instabilities in a dual-channel system. Comparing the outcomes of this study with White's (2011) findings and verifying the conclusion drawn by Lee and Pan (1999:32) was one of the objectives of the present study. The geometric configuration of the experiment (see Figure 2.1) was chosen based on the water reactor cooling concept (multiples of heat removal pipes).

The loop comprises three identical parallel channels, connected between a steam drum and header. A single down-comer, connected between two common plenums, i.e. the steam drum and header, provides the recirculation path. The steam drum forms the top plenum, while the header takes the bottom part of the setup to enforce natural circulation. The condenser was placed inside the steam drum to increase efficiency. Risers were electrically heated independently at the bottom by

means of heating elements. Heating the system at the bottom was chosen to accelerate the water-vapour mixture upward by buoyancy force into the steam drum, where cooling and separation of liquid and vapour will take place through gravitational settling.

The pressure drop was measured at the header using differential pressure sensors across the orifice flow meters. In addition, a pressure gauge was installed on the steam drum to measure the system's pressure. The steam drum was the preferred positioning of the pressure gauge because it is the highest part of the system, hence it will be easier to take pressure readings. The pressure gauge was also used to monitor the safety of the system during operation. As more heat is transferred into the system, pressure builds up and, if not monitored and engineered correctly, might lead to the system exploding. To ensure the safety of the system during operation, a safety valve was installed on the steam drum. The safety valve was set to operate when the pressure gauge reads greater than 110 kPa.

To relieve excess pressure build-up inside the experimental set up, the header was connected to an expansion tank open to the atmosphere. The expansion tank was connected to the header via a transparent pipe with a ball valve. It was decided to have a transparent expansion tank pipe so that the water level could be measured and expansion and contraction of the system could be observed. A ball valve was installed on the steam drum to evacuate air trapped inside the steam drum during system fill up. Two-phase flow is unstable in nature, hence a well-balanced holding frame was designed and built to hold the system (the four loops, expansion tank and steam drum) together, even under unstable events. Figure 2.1 shows a view of the experimental setup.

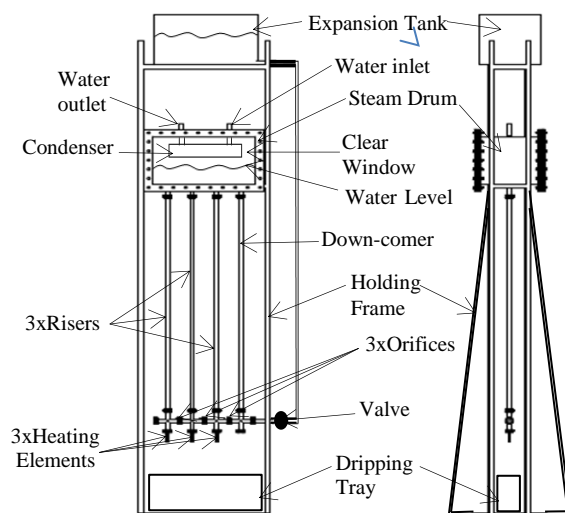


Figure 2.1: Experimental setup view

The geometric details of various components used in the experimental facility are shown in Table 1.

Table 1: Geometric Details of the System

Component	Dimensions (mm) and Orientation	Qty
Expansion Tank	400 w x 420 h x 700 L x 3 thick, Horizontal	1
Steam Drum	386 w x 400 h x 700 L x 3 thick, Horizontal	1
Condenser	200 w x 110 h x 400 L x 3 thick, including 7 x 28 OD x 3 thick x 290 L, Horizontal	1
Risers	28 OD x 3 thick x 1993 L, Vertical	3
Down-comer	28 OD x 3 thick x 1993 L, Vertical	1
Header	28 OD x 3 thick x 664 L, Horizontal	1
Orifice	30 OD x 12.5 ID x 2.5 thick	3
Heating elements	12.5 OD x 210 Cold L x 1000 Hot L, Vertical	3
Dripping Tray	794 w x 200 h x 1400 L x 1.6 thick, Horizontal	1
Holding frame	900 w x 4000 h x 1500 L, Vertical	1

To study the behaviour of a natural circulation flow, it was deemed necessary to visually observe the stability and instability of the flow during operation. To achieve this, the header, risers, down-comer, front and back sides of the steam drum were made out of transparent material (polycarbonate).

Thermal insulation was eliminated in the experimental setup because most of the system's components were purposely made transparent, and insulation would have blocked the view. The material and instruments used were selected based on certain engineering aspects, such as reducing thermal losses to the environment while meeting the desired purposes (clear view).

2.2. Experimental procedure

The experimental procedure started by filling the experimental set-up with water to the desired level in the steam drum (~100 mm) directly from the tap via the system's header. The system's header was then connected to the expansion tank open to the atmosphere to maintain the steam drum at constant pressure. The built-in pressure and visible air bubbles trapped in the system were released by opening the air release ball valve mounted on top of the steam drum. Air bubble dissipation was observed through the transparent channels and the steam drum's clear front and back views. The pressure gauge on top of the steam drum was also checked and monitored to ensure that it indicated

atmospheric pressure. The valve on top of the steam drum was then closed and heat was injected at full power into the system through the three heating elements inserted into the risers. The condenser was supplied with tap water at a constant flow rate to stabilise the steam drum pressure and cool the system.

Dissolved air onset was again observed with the increase in fluid temperature to close to boiling. The system was allowed to boil and all the trapped air and built-in pressure were removed by opening the steam drum-mounted valve. The system was maintained at boiling for a few minutes until steady state was reached and air bubble formation was no longer observed. The heat was then switched off and the system was allowed to cool down. This was done to ensure that the working fluid for the experimental tests was not contaminated by air.

It was also to ensure that no air was trapped in the steam drum, creating an air-blanket between the condenser and the working fluid, blocking the cooling of the system.

The safety of the experimental set-up and operation was ensured by putting up safety notices alerting other laboratory users to the dangers of the contrivance. All electrical appliances were visibly disconnected from the power supply after each test to minimise risks associated with fault currents. Another safety measure was to isolate the wet devices from the electrical equipment by housing the wet experimental system in a transparent protective frame.

Experiments

The experimental system was equipped with measuring instruments and connected to an Agilent® data acquisition unit with 20 input channels per card (it had three cards). The data acquisition unit was coupled with thermocouples and differential pressure sensors. The unit could allow data acquisition at scanning intervals of 1ms. Temperatures were measured in the steam drum, header, top and bottom of the risers and down-comer, inlet and outlet of the condenser and room temperature.

The pressure drop was measured between the risers and down-comer at the header section using differential pressure sensors. The maximum temperature error measurement was $(119.75\text{ °C} - 118.0\text{ °C}) = 1.75\text{ °C}$ and pressure measurement uncertainty was $((1 - 0.9789)/1) \times 100\% = 2\%$. After completing the preparations and safety checks, the experiments were performed.

The electrical heating elements were controlled independently using individual rheostats. At the

same time, the heating elements' power was gradually and independently increased in steps of approximately 200 W at a time. After the power rose to the desired value, the elements' power was maintained constant for nearly 30 min to ensure steady state was reached.

The natural circulation experimental investigation system was operated in three different modes, viz. open system, closed system and heat pipe mode. In the open system mode, the ball valve at the header was open so that the working fluid would expand to the expansion tank, therefore maintaining the system pressure at atmospheric pressure. For the closed system mode of operation, the expansion valve was closed and the steam drum pressure was maintained by the cooling system, the use of a safety valve and monitoring the pressure gauge to manually operate the air release valve if necessary. In the heat pipe mode of operation, the expansion valve was closed to maintain a constant volume, while the heating elements were switched off to suppress pressure increase and encourage boiling at low temperatures and pressures.

3. Numerical Modelling

For numerical modelling, transient one-dimensional conservation equations were derived from first principles for both single and two-phase fluids and used to program the system's discretized simulation model (Figure 3.1). The theory was developed by applying the equations of change, i.e. conservation of mass, momentum and energy, to an arbitrary control volume to produce difference equations to be used in a computer code. The derivation of the 1-D mathematical model was based on the following assumptions:

- Flow in the loops is one-dimensional
- Fluid flow is incompressible and the two-phase flow is homogeneous
- The Boussinesq approximation is valid
- The sub-cooled boiling effect is negligible
- The thermodynamic equilibrium is applicable to both phases, i.e. particle velocity \ll speed of sound
- Heat flux input is constant as the system is electrically heated
- Heat losses from the system (transparent plastic piping) to the environment are negligible
- Hydrostatic pressure along the bottom of the loop is constant

The above assumptions were collected from various successful research resources (Nayak et al., 2006:652; Yun et al., 2008:666; White, 2011:26; Goudarzi & Talebi, 2013:116) and used to simplify the conservation equation. The reason behind

considering each simplifying assumption is as follows: A one-dimensional method was used to model the experimental loop. This means that the working fluid properties varied in the axial direction of the flow tube only. Incompressible flow modelling means that there is no divergence in the fluid velocity, while homogeneous two-phase flow assumption implies that the liquid and vapour phases travel at the same velocity and the composition of water-vapour mixture is uniform and can be represented as a single fluid but with different properties.

Boussinesq approximation modelling assumes that the variation in inertia of the water-vapour mixture is negligible, but that the gravity is strong enough to differentiate the specific weights of the two fluids. Negligible sub-cooled boiling means the bubble formation during boiling would have insignificant impact on the flow rate. The thermodynamic equilibrium validity assumption implies that both phases would experience the same temperature instantaneously. Heat flux was assumed constant because heat addition into the system was done by electric heating rods. The effect of heat loss to the environment was assumed to be small such that it can be negligible, since polycarbonate material has fairly low thermal conductivity and most of the system parts were made from it. Pressure at the bottom of the loop (header) was assumed to be static, since natural circulation flows are usually low. Hence the header pressure was used as a pressure reference to simulate pressure at every point in the system.

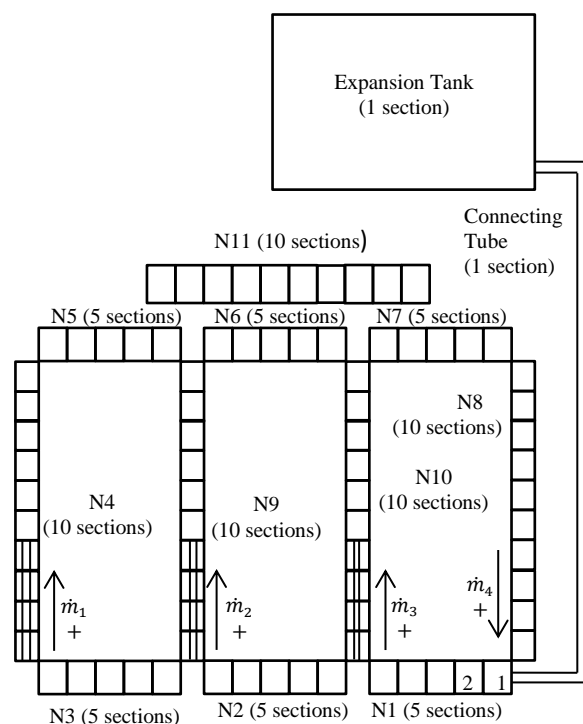


Figure 3.1: Discretized Experimental Model

3.1 Conservation of mass

The conservation of mass relation for a closed system undergoing a change requires that the mass of the system remains constant during the process. However, for a control volume, mass can cross the boundaries, as depicted in Figure 3.2

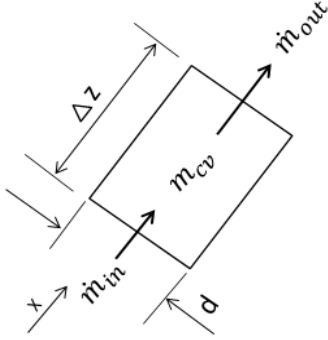


Figure 3.2: Fixed control volume for continuity

The change in mass with respect to time of the fixed control volume through which a fluid is flowing can be expressed simple as

$$\frac{\Delta m_{cv}}{\Delta t} = \dot{m}_{in} - \dot{m}_{out} \quad (1)$$

where \dot{m}_{in} and \dot{m}_{out} are the total rates of mass flow into and out of the control volume, and $(dm_{cv})/dt$ is the rate of change of mass within the control volume boundaries.

3.2 Conservation of momentum

Newton's second law states that the sum of all external forces acting on a system is equal to the time rate of change in linear momentum. Applying the Reynolds transport theorem to the system to formulate the system using control volumes, the general linear momentum equation (Cengel & Cimbala, 2006:234) can be expressed as

$$\sum \vec{F} = \frac{d}{dt} \int_{cv} \rho \vec{v} dv + \int_{cs,out} \rho \vec{v} (\vec{v}_r \cdot \vec{n}) dA_x - \int_{cs,in} \rho \vec{v} (\vec{v}_r \cdot \vec{n}) dA_x \quad (2)$$

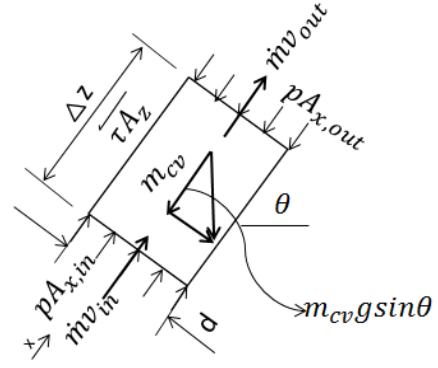


Figure 3.3: Fixed control volume for 1-D flow linear momentum

According to Cengel and Cimbala (2006:234), for a fixed control volume the fluid velocity relative to the control surface $(\vec{v}_r) = \vec{v}$, and then equation (3.2) becomes

$$\sum \vec{F} = \frac{d}{dt} \int_{cv} \rho \vec{v} dv + \int_{cs,out} \rho \vec{v} (\vec{v} \cdot \vec{n}) dA_x - \int_{cs,in} \rho \vec{v} (\vec{v} \cdot \vec{n}) dA_x \quad (3)$$

Applying equation (3) to the control volume in Figure 3.3, the term on the LHS of equation (3) becomes

$$\sum \vec{F} = pA_{x,in} - pA_{x,out} - \tau A_z - m_{cv} g \sin \theta \quad (4)$$

where $m_{cv} = \rho A_x \Delta z$, and substituting into equation (4) results in

$$\sum \vec{F} = pA_{x,in} - pA_{x,out} - \tau A_z - \rho A_x \Delta z g \sin \theta \quad (5)$$

The integral terms of equation (3) can be written in algebraic form on the assumption that density and average velocity across the control volume are nearly constant, hence ρ and v can be taken out of the integral, which results in

$$\Delta z \frac{\Delta(\dot{m})}{\Delta t} = pA_{x,in} - pA_{x,out} - \tau A_z - \rho A_x \Delta z g \sin \theta + (\dot{m}v)_{in} - (\dot{m}v)_{out} \quad (6)$$

Dividing equation (6) by A_x results in

$$\frac{\Delta z}{A_x} \frac{\Delta(\dot{m})}{\Delta t} = p_{in} - p_{out} - \tau \frac{A_z}{A_x} - \rho \Delta z g \sin \theta + \left(\frac{(\dot{m}v)_{in} - (\dot{m}v)_{out}}{A_x} \right) \quad (7)$$

Knowing that $-\Delta p = p_{in} - p_{out}$, and $v = \frac{\dot{m}}{\rho A_x}$, equation (7) becomes:

$$\frac{\Delta z \Delta(\dot{m})}{A_x \Delta t} = -\Delta p - \tau \frac{A_z}{A_x} - \rho \Delta z g \sin \theta + \frac{\dot{m}^2}{A_x} \left(\frac{1}{\rho A_{x,in}} - \frac{1}{\rho A_{x,out}} \right) \quad (8)$$

3.3 Conservation of energy

Cengel and Cimbala (2006:171) state that it is convenient to separate mechanical energy from thermal energy and to consider the conversion of mechanical energy to thermal energy as a result of frictional effects as mechanical energy loss. Then the energy equation becomes the mechanical energy balance. The conservation of energy principle requires that the net energy transfer to or from a system during a process be equal to the change in the energy content of the system. Consider the energy control volume in Figure 3. 4.

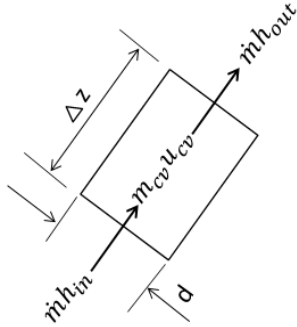


Figure 3.4: Energy control volume

Control volumes involve energy transfer via mass flow and the conservation of energy principle, also called the energy balance, is expressed as

$$\dot{E}_{in} - \dot{E}_{out} = \frac{dE_{cv}}{dt} \quad (9)$$

where \dot{E}_{in} and \dot{E}_{out} are the total rates of energy transfer into and out of the control volume respectively, and $\frac{dE_{cv}}{dt}$ is the rate of change of energy within the control volume boundaries.

According to Cengel and Cimbala (2006), the energy content of a fixed quantity of mass (a closed system) can be changed by two mechanisms, viz. heat transfer Q and work transfer W . For a fixed control volume, the energy equation can be expressed as

$$\dot{Q}_{net,in} + \dot{W}_{shaft,net,in} = \frac{d}{dt} \int_{cv} e \rho dV + \int_{cs} \left(\frac{p}{\rho} + e \right) \rho (\vec{v} \cdot \vec{n}) dA \quad (10)$$

In this study, $\dot{W}_{shaft,net,in} = 0$, no shaft is involved to drive the flow in the system, and then the energy equation becomes

$$\dot{Q}_{net,in} = \frac{d}{dt} \int_{cv} e \rho dV + \int_{cs} \left(\frac{p}{\rho} + e \right) \rho (\vec{v} \cdot \vec{n}) dA \quad (11)$$

Rewriting the second integral term in terms of average velocities and mass flow rates through the inlets and outlets, and assuming that $\left(\frac{p}{\rho} + e \right)$ is nearly uniform across the inlet and outlets, it can then be taken out of the integral (Cengel & Cimbala, 2006:205). Noting that $\dot{m} = \int_{A_x} \rho (\vec{v} \cdot \vec{n}) dA_x$ across the inlet and outlet, then equation (11) becomes

$$\dot{Q}_{net,in} = \frac{d}{dt} \int_{cv} e \rho dV + \left(\dot{m} \left(\frac{p}{\rho} + e \right) \right)_{out} - \left(\dot{m} \left(\frac{p}{\rho} + e \right) \right)_{in} \quad (12)$$

where $e = u + \frac{v^2}{2} + gz$, is the total energy per unit mass for both the control volume and the flow stream, and substituting back into equation (12) results in

$$\dot{Q}_{net,in} = \frac{d}{dt} \int_{cv} \left(u + \frac{v^2}{2} + gz \right) \rho dV + \left(\dot{m} \left(\frac{p}{\rho} + u + \frac{v^2}{2} + gz \right) \right)_{out} - \left(\dot{m} \left(\frac{p}{\rho} + u + \frac{v^2}{2} + gz \right) \right)_{in} \quad (13)$$

Fluid Properties

The thermodynamic properties of water and air were adapted from the appendices of Kröger (1998) according to White (2011:58), and this source offers enthalpy, density, etc., equations appropriate to use in a computer program.

Laminar Flow

For single-phase flow, the Darcy friction factor for laminar flow is given by Cengel and Cimbala (2006) as:

$$f_{lam} = \frac{64}{Re_d}$$

Darcy to Fanning conversion is given by Cengel and Cimbala (2006) as

$$c_f = \frac{16}{Re} \quad \text{for } Re < 1181$$

The Nusselt number for laminar fully-developed flow is adapted from Cengel (2006:468) as

$$Nu = \frac{hd}{k}$$

$Nu = 4.36$ laminar flow with (Cengel, 2006: 468)

Turbulence Flow

For the turbulence regime, the following options for friction factor were considered:

Blasius's equation (Cengel, 2006)

$f_{turb} = 0.316Re_d^{-0.25}$ $4000 \leq Re_d \leq 10^5$
 Filonenko's (1948) approximation of the Colebrook equation for smooth walls (White, 2011:58):

$$f_{turb} = (1.82 \log(Re_d) - 1.64)^{-2} \quad 4000 \leq Re_d \leq 10^{12}$$

Dobson (2014) and White (2011:58) recommended the Reynolds number at the transition point from laminar to turbulence to be taken as 1 181.

Colebrook's equation was used on the assumption that polycarbonate material is smooth (Cengel, 2006:867) and the fact that this equation was used to plot the Moody chart.

The minor losses coefficient was obtained from White (2011:59) and is given as

$$\tau_m = \rho \frac{v^2}{2} \Sigma K$$

The Nusselt number for turbulent flow is adapted from Cengel (2006:474) as

$$Nu = \frac{\left(\frac{f}{8}\right) (Re - 1000) Pr}{1 + 12.7 \left(\frac{f}{8}\right)^{0.5} (Pr^{2/3} - 1)}$$

According to Cengel (2007:474), this equation is more accurate.

Two-phase flow

For the two-phase flow, the void fraction concept was adapted. The vapour quality is given by

$$x = \frac{\dot{m}_g}{\dot{m}_g + \dot{m}_l}$$

Assuming that the two-phase mixture is homogenous, i.e. the velocity of each phase is the same, the density of the flow is adapted from Nayak et al. (2006:653) and White (2011:59).

$$\rho = \alpha \rho_v + (1 - \alpha) \rho_l$$

where α is the void fraction and is given as

$$\alpha = \left(1 + \frac{(1-x) \rho_v}{x \rho_l}\right)^{-1}$$

Substituting the void fraction back into the two-phase density equation results in

$$\rho = \left[\frac{x}{\rho_v} + \frac{1-x}{\rho_l}\right]^{-1}$$

Other two-phase flow properties, such as dynamic viscosity, specific heat and thermal conductivity, were adapted from Dobson and Ruppertsberg (2008:3), and are given below as respectively:

$$\mu = \left[\frac{x}{\mu_v} + \frac{1-x}{\mu_l}\right]^{-1}$$

$$c_p = x c_{p,v} + (1-x) c_{p,l} \quad k = \alpha k_v + (1-\alpha) k_l$$

The friction factor for two-phase flow was determined using the friction multiplier method and the Darcy to Fanning conversion $c_f = \frac{1}{4} f$.

$$f_{2\phi} = \phi_{lo}^2 f_{1\phi}$$

where White gives the friction multiplier as given by Whalley (1987:41, in White, 2011:59)

$$\phi_{lo}^2 = \frac{C_{fvo} \rho_l}{C_{flo} \rho_v}$$

This equation is claimed by White (2011:59) to be unrestricted in terms of applicability in the loop, where C_{fvo} and C_{flo} refer to coefficients of friction for vapour only and liquid only respectively.

The two-phase flow coefficient of friction was adapted from White (2011:60) for its simplicity and easy applicability in the program.

$$\frac{h}{h_{lo}} = (1-x)^{0.8} + \frac{3.8x^{0.76}(1-x)^{0.04}}{P_r^{0.38}}$$

where h_{lo} refers to liquid only heat transfer coefficient, x to the fluid quality and P_r to the reduced pressure, given by $P_r = p/p_{crit}$; p_{crit} is the critical pressure.

4 Solution algorithm

A computer code was developed, written and tested to predict the start-up transient and steady-state response of the natural circulation two-phase flow multichannel system. The computer code was developed from White's (2011) computer program, where he coded a dual loop parallel system for single and two-phase flow natural circulation. In this study, single- and two-phase flow natural circulation in a triple parallel channel and one down-comer system was programmed. The objective of the program was to predict the experimental behaviour (pressures, mass flow rates and temperatures) of the multichannel natural circulation loop, such that it could be evaluated against a specially designed and construct experimental loop.

The results of the simulation program were expected to possess reasonable comparison to the experimental outcomes. The following is a layout of the computer program's analysis.

Define arrays to store up to 99 numbers corresponding to the control volume in an array
 Define system constants such as thermodynamic properties and material properties

g = 9.81: PIE = 3.14159: Cp_g = 2094: Cv_g = 1564
 C_{pl} = 4226: h_{fg} = 2441700 '(@ 25degC, Cengel):

Cv1v = 4266: ufg = 2304300 '(@ 25degC, Cengel):
Pcrl = 2.212E7: rhowall = 1200: Cpw = 1260:
kwallpol=0.2: Cpwss = 468: rhowallss = 8238:
kwallss = 13.4

Define liquid properties and condenser dimensions
Wcw = 0.0363: Cpcw = 4180: Cvcw = 3718: IDcw =
= 0.394: ODcw = 0.025: ODc = 0.028: AXcw =
7*PIE * (ODcw ^ 2) / 4: Deqcw = (IDcw -
7*ODc):Lcw = 0.333: AZIDcw =
7*(Lcw*ODcw*PIE): AZODcw =
7*(Lcw*ODc*PIE): Twall = 0.0015: kwall = 401:
Cpwall = 385: rhowallcop =8933

Define system geometric grid dimensions

Define initial conditions such as initial temperature,
time step, atmospheric pressure, etc.

Vsupply = 230: DTIME = .05: time = 0: TSTEP = 0:
Tbegin = 21.0: Tcwi = 20: Ta = 23.7: Ttankbeg =
21: Patm = 100700: Rhot = 17.63

Define friction factors, environmental heat loss
factor, heat exchanger cooling factor, run time and
power factor

xf = 1 'friction
xl = 1 'environmental losses
xc = 1 'cooling
tm = 80 'run time in minutes
xp = 1 'power factor

Define the geometric dimensions of the expansion
tank

Ltank = .694: Btank = .394: Ztank = .2: Ptank = 2 *
(Ltank + Btank): Lpipe = 3.3: Dpipe = .025: Zpipe =
3.015: VOLg = 0: Ttank = Ttankbeg: Mtank =
fnRltemp(Ttank) * (Ltank * Btank * Ztank + PIE *
(Dpipe^2 / 4) * Lpipe)

Determine first cell hydrostatic pressure from
expansion tank open to the atmosphere

P1 = Patm + fnRltemp(Ttank) * g * (Zpipe + Ztank)
Calculate a cell's geometric properties around the
main loop

Calculate minor losses in pressure for each cell
located at tees, bends, contraction and expansions

Determine the initial cell interface pressures

Determine the initial average pressure and initial
saturation temperature

FOR k = 1 TO (N - N11)

PB(k) = ((P(k) + P(k + 1)) / 2)

Tsat(k) = fnTsatP(abs(PB(k)))

NEXT k

FOR k = (N - N11 + 1) to N

PB(k) = Patm + fnRltemp(T)*g*Zpipe

NEXT k

Assign initial temperatures and quality values to
each cell in the main loop. This assumes that there is
liquid only and no air and vapour in the system
initially.

FOR k = 0 TO (N - N11): T(k) = Tbegin: Twall(k) =
Tbegin: X(k) = 0: NEXT k

Calculate densities and mass flow rates of each cell

FOR k = 1 TO (N - N11)

Rg = fnRg(k): Rl = fnRl(k)

ALPHA(k) = fnALPHA(X(k))

R(k) = fnR(X(k), Rg, Rl)

M(k) = VOL(k) * R(k)

NEXT k

Calculate the cooling water cell temperatures and
masses

FOR k = (N - N11 + 1) to (N)

T(k) = Tcwi: Mcw(k) = fnRcw(k) * AXcw * L(k)

NEXT k

Calculate the net heat flows for each cell: the
program performs an energy balance for each cell
for each time step

Assign zero index values to each of the defined
arrays: this assures continuity from the beginning to
the end points in the loop

Give a warning to close the output text file

kill "LUCY_Test11.txt"

Open the output text file and write the heading titles,
program specifications, etc.

Open "LUCY_Test11.txt" for append as #1

Close the output file

close #1

START THE MAIN LOOP: Program returns to this
point after each time step's calculation

Initialise all four mass flow rates to zero

W1 = 0: W2 = 0: W3 = 0: W4 = Ws = 0

Run the simulation until the specified run time is
reached and then exit the loop and end the program.

[mainLoop]

IF time > (tm*60.0) THEN

GOTO [exitLoop]

END IF

Calculate each cell's new net heat flows for looping
purposes

Qcw5b = 0: Qcw6 = 0: Qcw7a = 0

if TSTEP mod 2000 = 0 then

print ""

end if

Assign mass flows to an array for passing to
functions

Assign outer heat transfer coefficients to an array

Determine enthalpies per cell

Determine heat lost to the wall to heat it up

for k = 1 to (N1 + N2 + N3 + N4a + N4b)

Twnew(k) = fnTw(k)

Qw(k) = Mw(k)*Cpw*(Twnew(k) - Twall(k))

next k

for k = (N1 + N2 + N3 + N4a + N4b + 1) to (N1 +
N2 + N3 + N4a + N4b + N5a + N5b + N6 + N7a +
N7b)

Twnew(k) = fnTw(k)

Qw(k) = Mw(k)*Cpwss*(Twnew(k) - Twall(k))

next k

for k = (N1 + N2 + N3 + N4a + N4b + N5a + N5b +
N6 + N7a + N7b + 1) to (N - N11)

Twnew(k) = fnTw(k)

Qw(k) = Mw(k)*Cpw*(Twnew(k) - Twall(k))

next k
Determine new cell temperatures and qualities
Calculate new densities for main cells
FOR k = 1 TO (N - N11)
Rg = fnRg(k): Rl = fnRl(k)
Rnew(k) = fnR(Xnew(k), Rg, Rl)
Mnew(k) = VOL(k) * Rnew(k)
ALPHAnew(k) = fnALPHA(Xnew(k))
NEXT k
Calculate new densities at the nodes
Calculate the internal energies from an energy balance and determine the new control volume qualities and temperatures
Determine the condenser's new inlet and outlet temperatures
Calculate new densities of the working fluid in the system
Determine new average expansion tank temperature
Determine new mass flow rates
Calculate the flow regime and governing friction model by

$$Re_D = \frac{4\dot{m}}{\pi\mu D}$$

if Re

< 2000 then the flow is laminar and the friction

$$\text{factor is } f = \frac{64}{Re} \text{ or}$$

if Re > 2000 then the flow is turbulence

$$f = \left[-1.8 \log \left(\frac{6.9}{Re_D} \right)^{-2} \right]$$

Calculate applicable constants for the differential equations
Calculate the full step equations
Calculate mass flow rates in each leg, using the full momentum equation as given by

$$\begin{aligned} \sum_{i=b}^k \frac{L_i}{A_{x,i}} \frac{\Delta \dot{m}_n}{\Delta t} = & - \sum_{i=b}^k \Delta p_i \\ & - 2 \sum_{i=b}^k \frac{L_i \dot{m}_n |\dot{m}_n|}{d_i \rho_i A_{x,i}^2} (C_{f,i} + K_{m,i}) \\ & - g \sum_{i=b}^k \rho_i L_i \sin(\theta_i) \\ & + \sum_{i=b}^k \frac{\dot{m}_n^2}{A_{x,i}} \left(\frac{1}{\rho_{i-1} A_{x,i-1}} - \frac{1}{\rho_i A_{x,i}} \right) \end{aligned}$$

Calculate new pressures at cell interfaces
Calculate new total pressures by determining friction, momentum and buoyancy pressures per cell
Based on the total cell pressures, calculate saturation temperatures at each cell
Calculate volumetric flow rates per leg by converting mass flow rates of each leg
Replace the old array values with the corresponding new system property arrays, to prepare for the new cycle
Print the key parameters to the output text file, including run times, mass flow rates, temperatures, etc.

Repeat all the steps in the main loop until total run time is reached
End the main loop
Define all functions to be called by the main program to perform calculations, such as function fnRltemp(T)
fnRltemp = (ar1 + ar2 * (T + 273.15) + ar3 * (T + 273.15) ^ 2 + ar4 * (T + 273.15) ^ 6 + 1e-3) ^ -1
end function

5 Results and discussion

Experimental and theoretical results were performed at various operation modes to study the behaviour of a two-phase natural circulation in a multi-parallel channel system. The three heating legs were subjected to equal power inputs simultaneously by independent electrical heating elements. The following sections describe the general observations from the experimental investigation.

5.1 Experimental observations

Experiments started by switching on the power, which triggered the development of natural circulation single-phase flow. The single-phase natural circulation was measured by the differential pressure sensors and could be observed through the transparent tubes. Single-phase flow natural circulation was observed as wave-front air with no air bubbles flowing along the loops (three risers connected to a common down-comer). The flow was evident, accelerating upwards through the risers after a few minutes of power injection. Two-phase flow was established at a channel power greater than 800 W. The increase in power and temperature of the working fluid resulted in the onset of air bubbles and increased pressure. The system was observed expanding and breathing through the expansion tank in the open system operating mode. The remaining air and built-in pressure were evacuated by opening the valve mounted on top of the steam drum, and this was also applicable to the closed system and heat pipe operation mode.

The two-phase flow open system operation mode went through three different flow regimes, viz. bubbly, slug and churn flow patterns. The interpretation of the flow patterns was adapted from Mills (1999:703). Only the bubbly flow regime was evident in the closed and heat pipe system operation modes. The power was maintained at the desired level in all three risers (heating elements) for at least 30 minutes for the system to reach steady state. Before the steady state was reached, a repeated sudden release series of voids pursued by a single-phase liquid was witnessed. During this phase the flow was oscillating widely and even reversed several times. Dissolved air trapped in the system was observed as bubbles accelerating into the steam

drum. The ventilation system mounted on top of the steam drum was operated repeatedly until there was no more visible air bubble formation.

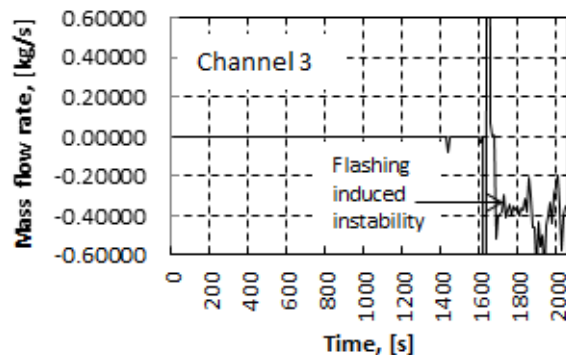
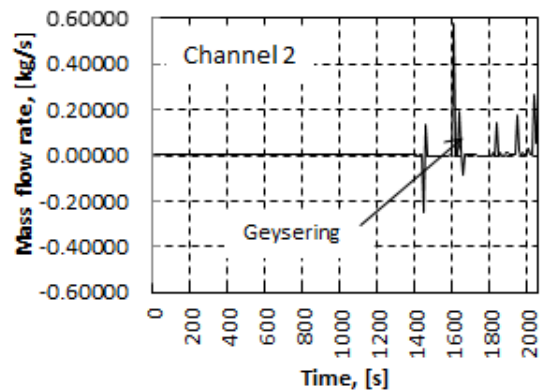
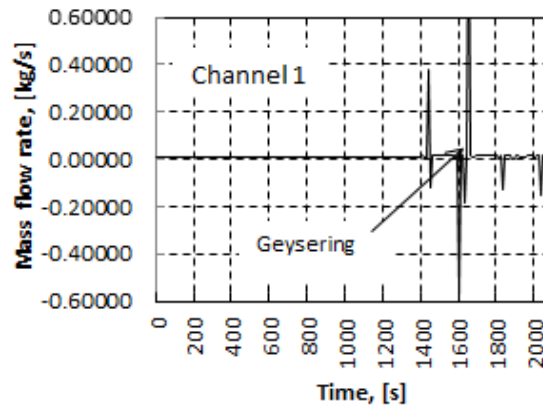
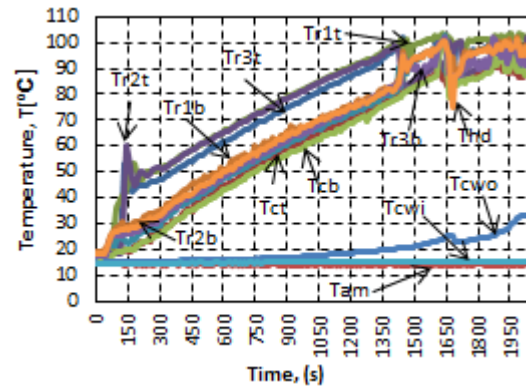
5.2 Experimental Results

The experimental system was operated as an open system, closed system and in heat pipe mode. The results obtained from all three operating modes are discussed in the following sections. The abbreviations in the temperature graphs are explained as follows:

- Tr1t - top temperature of the left riser
- Tr1b - bottom temperature of the left riser
- Tr2t - top temperature of the middle riser
- Tr2b - bottom temperature of the middle riser
- Tr3t - top temperature of the right riser
- Tr3b - bottom temperature of the right riser
- Tct - top temperature of the down-comer
- Tcb - bottom temperature of the down-comer
- Tcwo - outlet temperature of the cooling water
- Tcwi - inlet temperature of the cooling water
- Thd - Temperature at the header
- Tam - ambient temperature
- Tsd - steam drum surface temperature

Open expansion valve operating mode

In this mode the system was connected to the expansion tank open to the atmosphere. The condenser was connected to a cold water tap kept at a constant rate for the entire duration of the test. The water tap was initial fully open to evacuate air, if any, trapped in the condenser and to clear air bubbles. The condenser cooling water flow rate was then adjusted to the required flow rate (0.032 kg/s) and maintained for the entire duration of the experiment. The water outlet of the condenser was connected to a drain via a transparent plastic pipe. The mass flow rate of the cooling fluid was regularly checked by collecting the outlet water with a bucket while measuring time with a stop watch. The collected water was then weighed on a scale in kilograms and converted to kilograms per second. Experiments were performed over weekends when nobody was performing water activities that might cause disturbance in the cooling water flow rate while the experiment setup was in operation. The experimental open system operating mode results for the two-phase flow natural circulation in a multi-parallel channel system are presented below for the different power inputs.



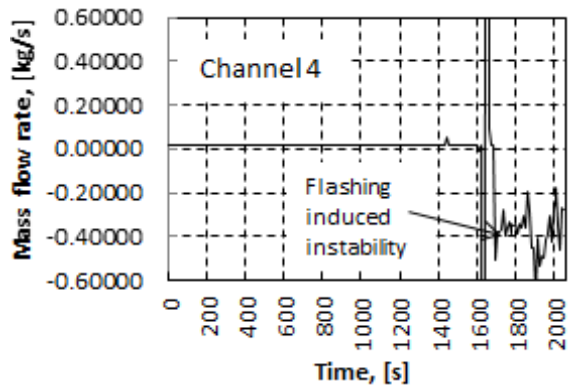


Figure 5.1: Temperatures and mass flow rate as a function of time of a 9kW (3kW per riser) test open system

The system's transient start-up response phase persisted no longer than 200 seconds, as is evident in Figure 5.1 (temperature graph). After friction was phased out, temperatures continued to rise slickly to 100 °C, where bubbly boiling commenced. During the rising mode of temperatures in the system (the first 1 400 seconds), the mass flow rates in all three risers were flowing in the positive direction, i.e. upward and coming down as a sum through the down-comer. Overshooting of a two-phase mass flow rate at the steady bubbly boiling condition was evident past 1 400 seconds (see Figure 5.1, channels 1, 2, 3 and 4). The mass flow rates in both channels 1 and 2 seemed to stabilise with occasional overshoots, whereas channel 3 was flowing in the reverse direction, causing the down-comer to flow in the opposite direction (upward) after 1 600 seconds.

Figure 5.1 shows that channels 1 and 2 were intermingling, while riser 3 and the down-comer possessed in-phase behaviour. It can be observed in Figure 5.1 that the continuous increase in power introduced flow oscillations in all the channels. It is evident from Figure 5.1 (temperature graph) that, during the oscillatory region the two-phase fluid was dominated with high quality since boiling is trending above 100 °C. It is can be seen from Figure 5.1 (channels 1 and 2) that a further increase in power resulted in the reduction of the amplitude of the oscillations. However, in channels 3 and 4, a continuous increase of power in the system resulted in flow reversal with reduced amplitude of the oscillations.

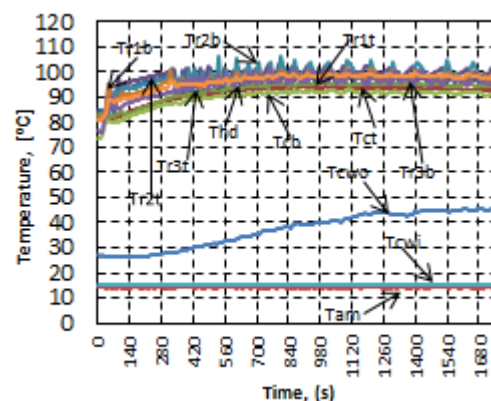
In this case, the flow compartment shifted from the buoyancy-dominated region to the friction-dominated phase. Under these operating conditions, the system encountered Type II instability, where high power gave rise to low flow rates due to high friction. Flashing instability in channels 3 and 4 was also observed as bottom riser temperatures approached top riser temperatures (header temperatures approached steam drum temperatures).

These kinds of instabilities were also observed by Jain et al. (2010) and Jiang et al. (1995) in their investigations of two-phase flow natural circulation systems.

Closed valve operating mode

After each open system test had reached steady-state conditions, the valve connecting the expansion tank to the system's header was closed and the power was switched off for a few minutes. This was done to settle down the system before operating it as a closed system. After the system had settled down, power was re-injected to the desired level to study the behaviour of a two-phase flow multi-parallel channel system. In this operation mode, the cooling water was maintained constant as in the operation mode for the open system. The water level was maintained at the same level (100 mm high in the steam drum) for all operation modes. Release of built-in pressure did not have a significant impact on the level of water in the system. A mark was made on the steam drum at 100 mm to ensure that the same level of water was maintained for all tests. The level of water was observed through the clear front and back parts of the steam drum.

This system operation (closed loop) possesses heat pipe features where the system is subjected to vacuum pressure, causing boiling to be achieved at low temperatures. The cooling system was active for the duration of this test to stabilise the pressure in the steam drum and prevent volumetric expansion. Temperature and mass flow rate data obtained during each time step under different power inputs are plotted and analysed in the following graphs.



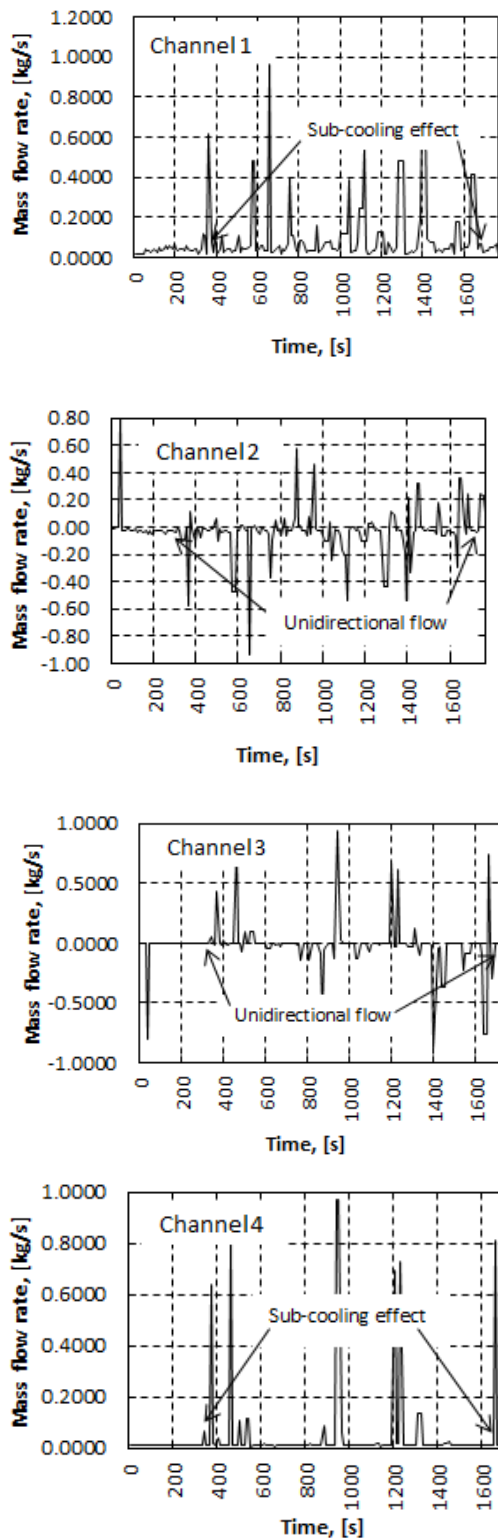


Figure 5.2: Temperatures and mass flow rate as a function of time of a 9kW (3kWper riser) test closed system

Operating the system with the expansion valve closed limited the start-up transient conditions to below 140 seconds. At this operating condition (closed system), the temperature rose rather rapidly from 75 °C, reaching stability at approximately 350

seconds after a minor overshoot. The system maintained steady-state temperature conditions for the entire duration of the test after that. It is clear from Figure 5.2 (temperature graph) that the top temperatures of the risers were fluctuating around 100 °C, hitting 105°C at times, while the cooling system's outlet temperature rose noticeably and settled just above 45°C. The mass flow rates in Figure 5.2 (channels 1, 2, 3 and 4) show that the fluid movement was stable but with periodic oscillations, unlike at low and medium-power operating conditions, when oscillations were not so severe.

Interaction between channels 2 and 3 can be witnessed in Figure 5.2 (channels 2 and 3), which shows that the flow rates in channel 2 and 3 were low on average, with back and forth (forward and reverse flow) overshoots. The actions of channel 2 affected the flow and stability of channel 3. Similar conduct between riser 1 and the down-comer's mass flow rates can also be noted in Figure 5.2 (channels 1 and 4). Channels 2 and 3 were general flowing in the reverse direction, while channel 3 and the down-comer remained in the forward flow direction (see Figure 5.2, channels 1, 2, 3 and 4).

Channels 1 and 4 were buoyancy dominated, while channels 2 and 3 were unidirectional with mixed-mode oscillations with a further increase in temperature. The average magnitude of the mass flow rate did not change after closing the valve, but definitely increased the amplitude of the oscillations. It is evident from Figure 5.2 that the flow was pulsating as the quality of fluid increases (vapour generation), which caused periodic oscillations with high peaks. Vibrations were minimised rigorously and the manageability of the system was acquired quicker under this operating condition.

Heat pipe mode

In this operation, the valve connecting the experimental setup with the expansion tank open to the atmosphere was closed. The cooling was initially switched off and the ventilation system was opened to release built-in pressure and steam as the power was progressively increased. The system was powered at 9 kW and maintained for at least 30 minutes. The flow started as a single-phase smooth flow and transited to two-phase flow as heat was continuously injected into the system. The system was heated continuously until boiling point was reached. This was evident by the steam escaping in the ventilation system. Steam was allowed to escape for some time to relieve the system of pressure build-up and air stemming from liquid breakdown. The pressure gauge was monitored constantly for any increase in pressure to beyond atmospheric pressure. No rise was observed in the pressure gauge

after the ventilation system was opened to maintain the system at atmospheric pressure during power increases.

After steady boiling was ascertained, the power and ventilation system were simultaneously switched off. At the same time cooling was turned on at full rate from the water tap to rapidly cool the system. At this point, bubbly boiling of the water in the steam drum was observed and the entire system was experiencing the bubbly boiling regime. The pressure gauge mounted on the steam drum indicated a gradual pressure drop to below atmospheric pressure. Bubbly boiling continued in all the channels and the steam drum while pressure continued to fall to minus one (-1) bar. After the pressure in the system had reached -1 bar, it rose gradually while boiling was uninterrupted. Bubbly boiling in the system stopped when the pressure gauge indicated minus half (-1/2) bar in rising mode.

Temperatures and pressure drops were measured using thermocouples and differential pressure sensors. Data was captured using an Agilent data acquisition unit and plotted in the figures below for further analysis.

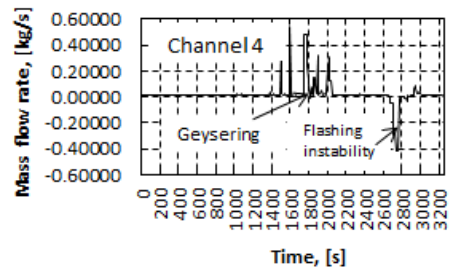
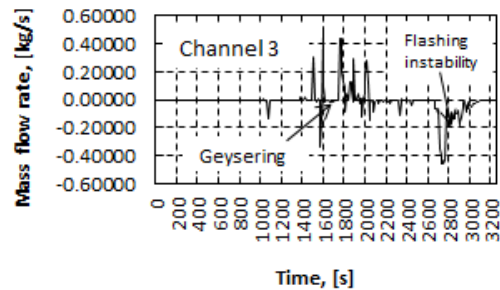
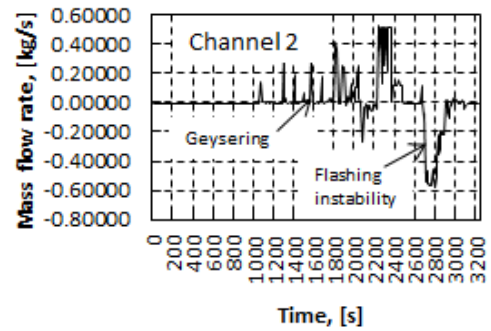
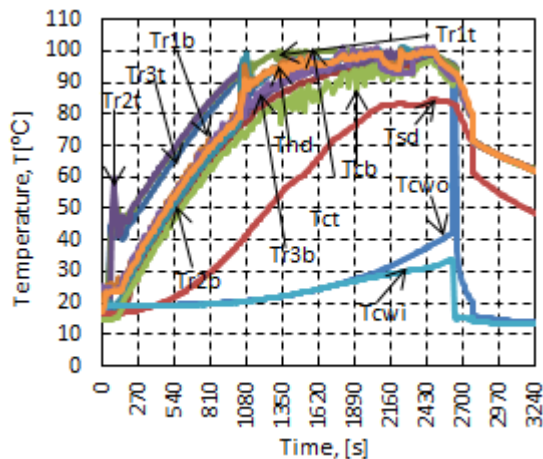


Figure 5.3: Temperatures and mass flow rate as a function of time of a 9kW (3kW per riser) test heat pipe mode operation

For heat pipe mode operation the system was powered at 3 x 3 kW for the intervals as explained above. Under this condition a typical transient start-up response was noticed in approximately the first 50 to 150 seconds when, after overcoming friction, the system's temperature rose sufficiently. Figure 5.15 shows that a minor overpass was experienced at approximately 1 080 seconds before the two-phase flow reached stability, with a maximum temperature of 100°C. The system maintained boiling at steady conditions without cooling being turned on. The power and ventilation system were then both switched off and cooling was simultaneously turned on at 1 890 seconds and the entire system started bubbly boiling instantaneously.

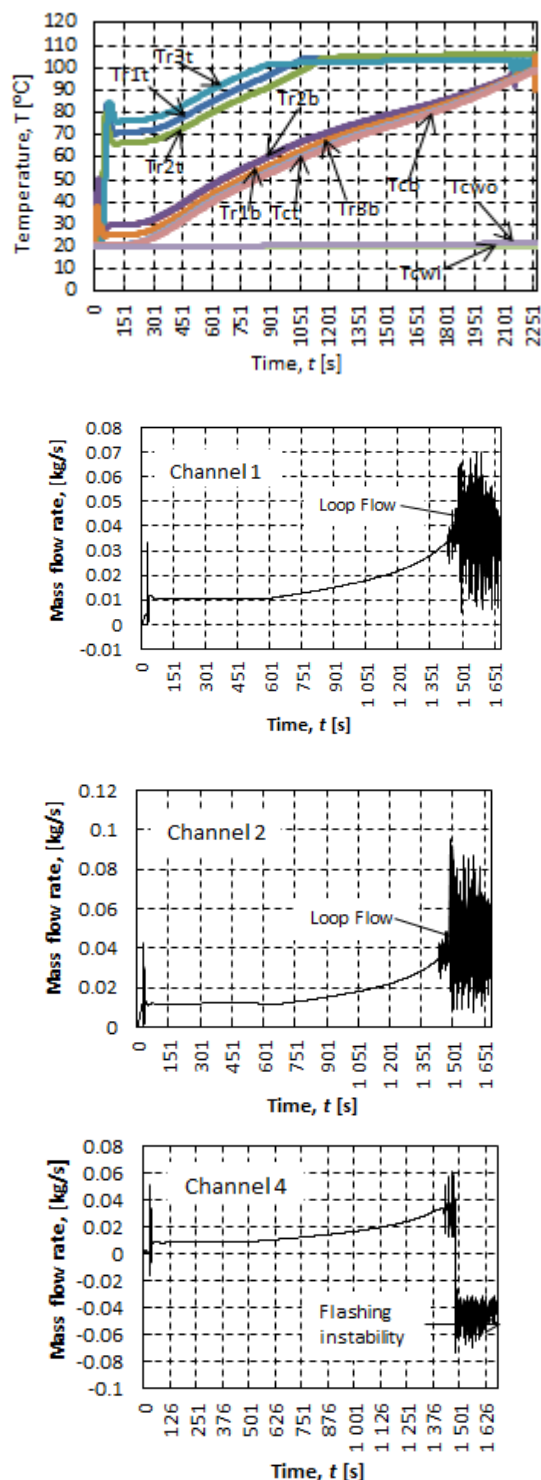
The cooling system (water-cooled condenser) removed heat rapidly from the experimental set-up, dropping temperatures severely and maintaining pressure in the steam drum. Under this condition (heat pipe mode), the system sustained bubbly boiling even at low temperatures (approximately 65°C). Boiling ceased when temperatures fell to below 60°C.

Figure 5.3 (channels 1, 2, 3 and 4) shows that the fluid was initially flowing smoothly in all four channels in a forward direction. The smooth flow was terminated shortly after the overshoot at 1 080 seconds and bubbly boiling commenced thereafter. The sudden introduction of oscillations materialised from an additional buoyancy force in the system due to a continuous increase in temperature. The two-phase flow rates become chaotic, with occasional reversal mode in all channels during the bubbly boiling phase. This mass flow rate conduct was sustained even at low temperatures. According to the mass flow rate graphs, there was a robust interaction (out-of-phase) between the fluid flow of riser 1 and 2, whereas channel 3 and the down-comer (channel 4) experienced a sudden shift from out of phase to in phase.

The heat pipe mode operation possessed Type II geysering and flashing-induced instabilities. Type II instability is associated with high power operation and steam void formation, as explained in the previous sections. Flashing instability materialised from the combination of high power and increased inlet (bottom) temperatures. Geysering instability resulted from the system operating with low pressure and low steam quality. For heat pipe mode operation, the system was functioning at pressures below atmospheric pressure and boiling was established at temperatures below 100°C. The quality of steam generated was fairly low due to the low system pressure. These kinds of instabilities in a two-phase natural circulation system operated at low pressure were also witnessed by Jiang et al. (1995) and Marcel et al. (2010).

5.3 Theoretical results

One of the objectives of this study was to develop a computer program that would simulate the two-phase flow response in a multi-parallel channel system. The program was developed and tested using the same inputs as the experimental setup. The geometric configuration and material properties of the experimental investigations were also used in the simulation code. The reasoning behind the development of the program was for one to be able to predict the comportment of a passive two-phase flow system and make reasonable engineering decisions without conducting experimental investigations. The sequencer was simulated to provide temperature and mass flow rate data for each time step exploited from the locations, as indicated in Figure 5.4.



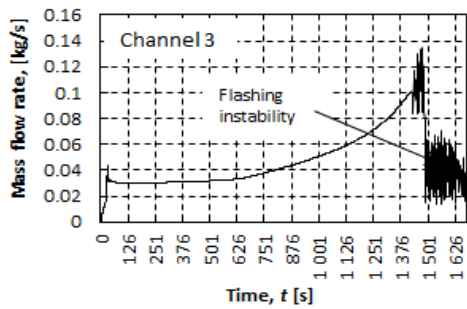


Figure 5.4: Temperatures and mass flow rate as a function of time of a 9kW (3kWper riser) test heat pipe mode operation

The transient start-up response duration reduced to nearly 75 seconds (see Figures 5.4). After overcoming friction, the temperatures dropped slightly and rose efficiently, with the risers' top temperatures reaching steady-state conditions at roughly 670 seconds. The bottom temperatures of the risers and down-comer rose effortlessly beyond 90°C, after which channel 3's top temperature started showing minor instabilities due to the entire system reaching bubbly boiling and sub-cooled boiling rising fast into the steam drum through channel 3.

The mass flow rate graphs (Figure 5.4, channels 1, 2, 3 and 4) show that the two-phase fluid was flowing at a constant rate of approximately 0.01 kg/s in all the channels after disabling friction. The constant circulation rate started increasing forcefully shortly after the risers' top temperatures reached stability at 670 seconds. After the bottom temperatures of the risers increased past 90°C, the mass flow rates became oscillatory in all channels, with riser 3 flowing in the reverse direction. In this region the system was undergoing flashing-induced instability. At this phase, the down-comer's mass flow rate fell, but it maintained its forward directional flow. This simulation test possessed Type II instability, where the continuous increase in power generated a buoyancy force, which later created reverse flow in channel 3.

Figure 5.4 show that channels 1 and 2 possessed similar mass flow rate demeanour (in-phase), while channel 3 and the down-comer responded in the same manner (in phase). Similar conduct was also observed in the experimental test operated as an open system powered at 9 kW. It is interesting to see that the channels do not necessarily assume the same behaviour, even if they are heated equally. It is further noted that increasing power does not necessarily increase average flow rate.

6 Conclusions

This study examined the start-up transient and steady-state response of a two-phase fluid natural circulation in a multi-parallel channel system. A

three parallel loop system was designed, built and used to perform the practical investigations. A one-dimensional computer program was also coded to study the response of the test facility subjected to various power inputs at constant pressure (atmospheric). It is evident from the experimental investigations of this study that heat transfer into a fluid results in water breakdown and air materialisation, no matter how airtight the system is. This was also encountered by Vyas et al. (2010) in their investigations in which demineralised water was used. Hence, a pressure release and air ventilation system is a basic requirement of any system undergoing heat addition. The simulation model predictions were validated with the experimental observations.

Investigations were carried out over a range of process parameters, i.e. varying power inputs and operation modes under two-phase natural circulation. At least four kinds of instability were observed in this study from different operating factors. Type I instability, Type II instability, geysering and flashing instability were the instabilities encountered in this investigation. Open system operation mode possessed start-up transient responses that lasted longer compared to the closed system mode of operation. Geysering instability and out-of-phase periodical oscillations between adjacent channels were commonly observed for all the open system natural circulation power excitations. The existence of flashing instability accompanied by mechanical vibrations at high inlet temperatures was one of the instabilities encountered at high power excitation in an open system. Lakshmanan and Manmahan (2010) discovered the same instabilities in their experimental and numerical investigations in parallel-channel natural circulation boiling systems.

Transient duration varied with power system operation modes and hence the stability of the system. A rise in power proved not to necessarily increase fluid mass flow rate but invited oscillations with higher amplitudes depending on the system's mode of operation. Type-I instability and low quality steam oscillations were witnessed at low power and open system operation mode (expansion tank valve opened). Type-II instabilities and flashing instability were observed to be associated with medium and high power excitations for open system mode of operation.

The fluid flow became more stable and less oscillatory at all power excitations for closed system (expansion tank valve closed) operation mode. However, a/the sub-cooling effect was evident at higher power where the two-phase fluid temperatures oscillated in a sinusoidal-like manner. Whereas, the mass flow rates oscillated with high

amplitudes in the forward direction in some channels and assumed a unidirectional flow in other channels.

In general, steady state conditions were obtained earlier when the system was operated as a closed system. For heat pipe mode of operation, the system transient response exhibited geysering instability followed by flashing induced boiling in all channels. In-phase (similar) and out-of-phase (opposite) behaviors between adjacent channels were experimentally observed at all power excitations and system operation modes. Flow reversal in heated channels of a natural circulation system proved to exist even under equal power excitations.

The results obtained through the numerical model were compared to the experimental results and discovered to have reasonable correlation. Both experimental and numerical results were also compared to results from similar work done by other researchers (Jain et al. (2010), Yun et al. (2008), and Marcel et al. (2010)) and were found to be in good agreement.

Acknowledgements

The authors thank the South African Heat Pipe Association (SAHPA[®]) for funding this work.

References:

1. Cengel Y.A. 2006. Heat and mass transfer: A practical approach, 3rd ed., New York: McGraw-Hill.
2. Cengel Y.A. & Cimbala J.M. 2006. Fluid mechanics: Fundamentals and applications, 1st ed., New York: McGraw-Hill.
3. Goudarzi N. & Talebi S. 2013. Linear stability of a double-channel two-phase natural circulation loop. *Progress in Nuclear Energy*. 67 (2013): 114-123.
4. Jain V., Nayak A.K., Vijayan P.K., Saha D., Sinha R.K. Experimental investigations on the flow instability behaviour of a multi-channel boiling natural circulation loop at low-pressures. *Experimental Thermal and Fluid Science*, No. 34, 2010, pp.776-787.
5. Jiang S.Y., Yao M.S., Bo J.H., Wu S.R. 1995. Experimental simulation study on start-up of the 5MW nuclear heating reactor. *Nuclear Engineering and Design*. 158 (1995): 111-123.
6. Kröger D.G. 1998. Air-cooled heat exchangers and cooling towers: Thermal flow performance evaluation and design. Stellenbosch: Stellenbosch University.
7. Lakshmanan S.P. & Pandey M. 2010. Numerical investigations of startup instabilities in parallel-channel natural circulation boiling systems. *Science and Technology of Nuclear Installations*. 2010: 1-8.
8. Lee J.D. & Pan C. 1999. Dynamics of multiple parallel boiling channel systems with forced flows. *Nuclear Engineering and Design*. 192 (1999):31-44.
9. Marcel C.P., Rohde M., Van Der Hagen T.H.J.J. *Experimental investigations on flashing induced instabilities in one and two-parallel channels: A comparative study*. *Experimental Thermal and Fluid Science*, No. 34, 2010, pp. 879-892.
10. Mills A. F. 1999. Heat transfer, 2nd ed., Prentice Hall, Upper Saddle River.
11. Nayak A.K., Lathouwers D., Van der Hagen T.H.J.J., Schrauwen F., Molenaar P., Rogers A. 2006. A numerical study of boiling flow instability of a reactor thermosyphon system. *Applied Thermal Engineering*. 26 (2006): 644-653.
12. Ruppertsberg J.C. 2008. Transient modelling of a loop thermosyphon. MScEng thesis. Stellenbosch. Stellenbosch University.
13. Swapnalee B.T. & Vijayan P.K. *A generalized flow equation for single phase natural circulation loops obeying multiple friction laws*. *International Journal of Heat and Mass Transfer*, No. 54, 2011, pp. 2618-2629.
14. Vyas H.P., Raj V.V., Nayak A.K. 2010. Experimental investigations on steady state natural circulation behavior of multiple parallel boiling channel system. *Nuclear Engineering and Design*. 240 (2010): 3862-3867.
- White H.A. 2011. Investigating instabilities in a multi-channel thermosyphon Loop. Final-year project. Stellenbosch. University of Stellenbosch.
15. Yun G., Qiu S.Z., Su G.H., Jia D.N. *Theoretical investigations on two-phase flow instability in parallel multichannel system*. *Annals of Nuclear Energy*, No. 35, 2008, pp. 665-676.
16. Zhang Y.J., Su G.H., Yang X.B., Qiu S.Z. *Theoretical research on two-phase flow instability in parallel channels*. *Nuclear Engineering and Design*, Vol. 239, 2009, pp. 1-10.